Er$_{1-y}$Ca$_y$Ba$_2$Cu$_{3-x}$(Fe, Zn)$_x$O$_{7-\delta}$ superconductors: a study of microstructure and resistive transitions in a dc magnetic field

Anurag Gupta[1], Sukalpa Chaudhuri[1,4], V Ganesan[2], I Das[2], H Narayan[1], Anil Kumar[1], A J Zaleski[3] and A V Narlikar[1,5]

[1] National Physical Laboratory, K S Krishnan Road, New Delhi 110012, India
[2] Inter-University Consortium for DAE Facilities, Khandwa Road, Indore, India
[3] Institute of Low Temperature and Structural Research, 50-950 Wroclaw 2, Poland

Abstract
We report an investigation of structure by x-ray diffraction, microstructure
by atomic force microscopy (AFM) and broadening of resistive transitions
in high dc magnetic fields (0–20 kOe) in Er$_{1-y}$Ca$_y$Ba$_2$Cu$_{3-x}$(Fe, Zn)$_x$O$_{7-\delta}$
($y = 0.1, 0.2$; and $0 \leqslant x \leqslant 0.20$) ceramic superconductors. The XRD
shows that the presence of Ca does not alter the known effect of Fe/Zn
substitution on the structure of the pure ($y = 0$) system. Substitution of both
Fe and Zn leads to a decrease in the grain size and micro-hardness.
Interesting results were obtained on the influence of various dopants on the
broadening of resistive transitions in dc magnetic fields, in general: (1) an
increase in Ca content suppresses it; (2) Zn substitution has no effect; and
(3) Fe substitution enhances it. We show that these results can be interpreted
in terms of a thermally activated flux motion (TAFM), and the effect of
various dopants on the properties like pinning barrier and anisotropy.

(Some figures in this article are in colour only in the electronic version)

1. Introduction

Disorder in high-temperature superconductors (HTSCs),
produced by naturally occurring defects (such as twin
boundaries, growth defects, normal precipitates and grain
boundaries) or produced artificially (for example point and
line defects) by irradiation of energetic light and heavy
particles, are known to contribute to the flux line lattice (FLL)
dynamics [1, 2]. Cationic substitutions may also give rise to
disorder and/or change in the electronic structure. Both these
effects, besides their influence on superconducting critical
temperatures [3–5], may play an equally important role in
determining the critical current density or, generally, the FLL
dynamics in HTSCs [6–8]. Recently [9], Ca-doped Y-123

systems have been shown to be of particular interest for such
investigations. In the present work we report the effect of
Fe/Zn (at Cu-sites) substitutions in Ca-doped (at an RE site,
RE ≡ Rare Earth) REBa$_2$Cu$_3$O$_{7-\delta}$ (i.e. RE-123) system on
structure, grain size, micro-hardness and FLL dynamics. We
show that these substitutions have a tangible presence in all
such properties.

2. Experimental details

A series of compounds having the composition Er$_{1-y}$Ca$_y$Ba$_2$-
Cu$_{3-x}$(Fe, Zn)$_x$O$_{7-\delta}$ (i.e. Er(Ca)-123) where $y = 0.1, 0.2$ and
$x = 0, 0.05, 0.10, 0.15, 0.20$ were prepared by the solid state
route under identical conditions. Stoichiometric quantities of
finely powdered Er$_2$O$_3$, BaCO$_3$, CuO and Fe$_2$O$_3$ (ZnO) of high
purity (99.99%) were mixed and ground in a mortar and pestle
manually for about 30 min until a roughly homogenous mixture
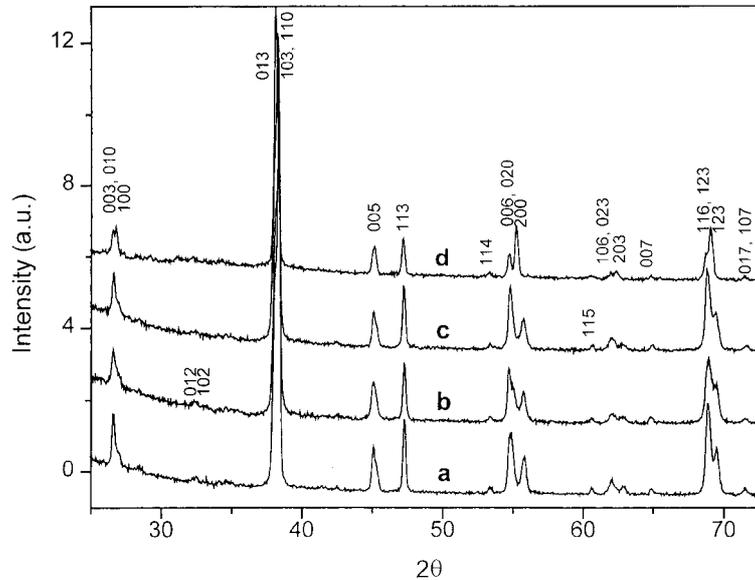
Figure 1. X-ray diffraction patterns of $Er_{1-y}Ca_yBa_2Cu_{3-x}(Fe, Zn)_xO_{7-\delta}$ samples: (a) $y = 0.1$, $x = 0$; (b) $y = 0.2$, $x = 0$; (c) $y = 0.1$, $x = 0.2$ (Zn); and (d) $y = 0.1$, $x = 0.2$ (Fe).

was formed. The mixture is then placed in alumina boats and calcined in air at 870 °C for 24 h. Next this reacted power is reground and reheated at 880 °C for a further 24 h. The resulting powder is finally reground and reheated to 890 °C for another 24 h. The black powder obtained is pulverized and cold-pressed into pellets which are sintered at 940 °C for 24 h in an oxygen atmosphere followed by slow cooling to room temperature. To obtain oxygenated samples, these pellets were annealed under an oxygen flow at 500 °C for 24 h in the last run.

All the samples were characterized for their phase purity by x-ray diffraction (XRD) using Co radiation with $\lambda = 1.788\,92$ Å. An atomic force microscope (AFM) (Nanoscope II), operating at ambient temperature in non-contact mode, was employed to study the changes in the microstructure due to Fe/Zn doping in the series of samples with $y = 0.2$. The series of samples with $y = 0.1$ were used to study the effect of Fe/Zn doping on hardness, which was measured by a micro-hardness system based on the Vickers hardness scale. Four probe resistance $R(T, B)$ measurements of all samples were performed in dc magnetic fields ranging from $B = 0$–20 kOe and a temperature range of $T = 10$–100 K. Parallelpiped-shaped samples, typically of length = 7–9 mm, width = 2–4 mm and thickness = 1–2 mm, were used for the $R(T, B)$ measurements. The current density was kept less than 10 mA cm^{-2} and the current direction was perpendicular to B.

3. Results and discussion

3.1. XRD

All the samples were found to be single phase. The XRD patterns for a few selected samples are reproduced in figure 1. In all cases, the XRD peaks could be well identified with the expected pattern of the known orthorhombic/tetragonal pure RE-123 system [3, 4]. With Ca substitution in the Er(Ca)-123 system the orthorhombicity is retained. This can be clearly

deduced from the observed splitting and relative intensity of the (020, 200) and (123, 213) reflections occurring at 55° and 69° (see figure 1 (patterns a and b)), respectively [10]. With the substitution of Zn (for $x = 0.2$, see figure 1, pattern c) no change is observed in the orthorhombicity, whereas substitution of Fe, for $x \geqslant 0.1$, leads to a structural transformation from orthorhombic to tetragonal. A reversal of the relative intensity in the doublets occurring at 55° and 69° in figure 1, pattern d, as compared to other patterns in the same figure, reveals [10] such a transformation in the $x = 0.2$ Fe-doped sample. These results corroborate well with those reported previously on Zn/Fe substitution in a pure ($y = 0$) Ca-free R-123 system [3, 4]. Thus, the presence of Ca in the Er-123 system does not alter the effect of Fe or Zn substitution on its structure.

3.2. Grain size and micro-hardness

The AFM photographs of five different samples of the series $y = 0.2$ with varying Fe/Zn content are shown in figures 2(a)–(e). With increasing Fe/Zn content in Er(Ca)-123 a decrease in grain size is observed. The decrease is much more prominent in the case of Fe, where the grain size decreases from an average of 0.3 μm to 0.03 μm for an increase in Fe content from $x = 0$ to 0.2, respectively. In the case of Zn, for the same increase in content, the decrease is from an average of 0.3–0.1 μm. These results reflect the different growth kinetics of Er-123 ceramics in the presence of Fe or Zn.

The dependence of micro-hardness on Fe/Zn substitution in samples of $y = 0.1$ series is shown in figure 3. As seen from the figure the micro-hardness decreases with an increase in both Fe and Zn content in the Er(Ca)-123 system. These results suggest that Fe/Zn substitution changes the material strength. If the material had remained the same, with only the grain size as the influencing parameter, the micro-hardness should, in fact, have increased in both cases, which is not observed.

(a)

(b)

(c)

(d)

(e)
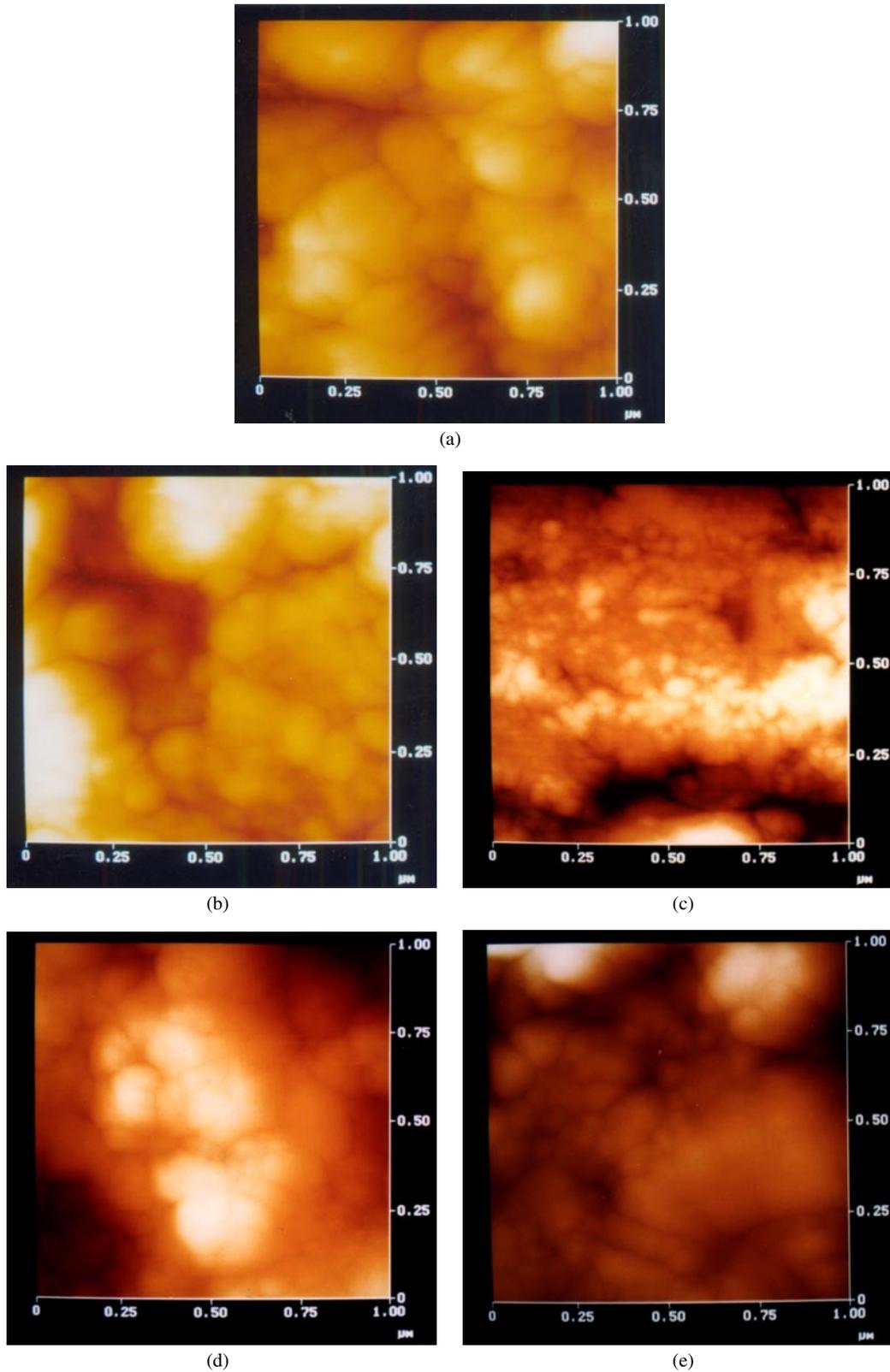
Figure 2. AFM photographs of Er$_{0.8}$Ca$_{0.2}$Ba$_2$Cu$_{3-x}$(Fe, Zn)$_x$O$_{7-\delta}$ samples: (a) $x = 0$; (b) $x = 0.1$ (Fe); (c) $x = 0.2$ (Fe); (d) $x = 0.05$ (Zn); and (e) $x = 0.2$ (Zn).

3.3. Resistive transitions in magnetic field

Figure 4 shows the resistance as a function of temperature in the presence of different applied dc magnetic fields ranging from 0–20 kOe. Four different samples with different Ca and/or Fe/Zn content are depicted in figures 4(a)–(d). At $B = 0$ we note that, for Fe/Zn-free ($x = 0$) samples, Ca substitution
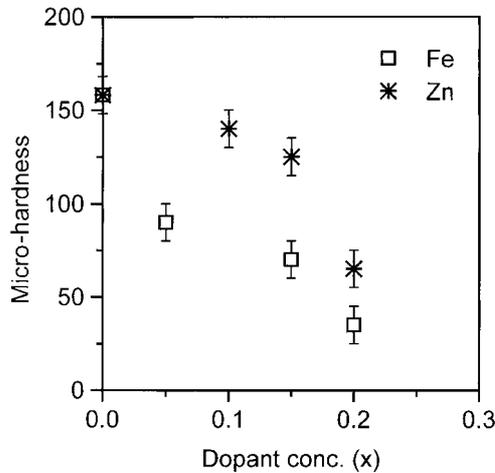
Figure 3. Micro-hardness as a function of Fe/Zn content in $Er_{0.9}Ca_{0.1}Ba_2Cu_{3-x}(Fe, Zn)_xO_{7-\delta}$.

suppresses the $T_c(R = 0)$ from ∼77 K (for $y = 0.1$) to ∼65 K (for $y = 0.2$). The observed decrease in T_c with increasing Ca content in the Er-123 system is similar to that reported earlier [9, 20]. In the presence of a magnetic field the resistive transition temperature ($T^*(B)$, defined as the temperature where $R \approx 0$), for the ($y = 0.1$, $x = 0$) sample, shifts to a lower temperature by ∼12 K (see figure 4(a)) when B increases from 0 to 20 kOe. However, in the case of the ($y = 0.2$, $x = 0$) sample, for a similar change in the field the shift $T^*(R \approx 0)$ is only ∼8 K (see figure 4(b)). The broadening of the resistive transition in dc magnetic fields has been attributed to thermally activated flux motion (TAFM); $R(T)$ may be given by $R \propto \exp(-U_b/kT)$, where U_b is related to the pinning barrier [11, 12]. The results in figures 4(a) and (b) may thus demonstrate that with increasing Ca substitution the pinning barrier increases, which results in a suppression of TAFM in the Er(Ca)-123 system.

Now we discuss the $R(T)$ curves for the Fe/Zn-substituted Er(Ca)-123 system, see figures 4(c) and (d). In the presence of Ca, the Zn substitution suppresses T_c from ∼77 K ($y = 0.1$, $x = 0$) to ∼44 K ($y = 0.1$, $x = 0.15$), whereas, in contrast, the substitution of Fe does not affect the T_c severely, which changes from ∼77 K ($y = 0.1$, $x = 0$) to ∼73 K ($y = 0.1$, $x = 0.15$). We will not go into the details of the zero-field results, which will be presented elsewhere as a separate communication. However, as seen from figures 4(c) and 4(d), in the presence of magnetic field the Fe-substituted samples show considerable TAFM compared to that for Zn samples. For a more comprehensive and quantitative view, we plot the shift in $T^*(B)$, i.e. $T^*(B = 0) - T^*(B = 2)$ as a function of Fe/Zn content for both the $y = 0.1$ and 0.2 series in figure 5. Several interesting observations can be made from this figure. First, for both these series of samples and for any value of x, the shift in T^* is larger in the case of the Fe-substituted samples than in the Zn-substituted samples. Second, for both series of samples, the shift in T^* rises monotonically with increasing Fe content, whereas, for Zn the shift in T^* is nearly unaffected by a change in Zn content. These results clearly indicate that substitution of Fe enhances TAFM in Er(Ca)-123. In contrast Zn substitution has no effect on TAFM in Er(Ca)-123. The origin of this could be

that, in the former case, substitution (Fe) at the Cu(1) site in Cu–O chains makes the Er(Ca)-123 system more anisotropic, whereas substitution (Zn) at the Cu(2) site in the CuO_2 planes does not affect the anisotropy. A similar conclusion was reached in [13], where Fe substitution was shown to reduce the coupling between the CuO_2 planes in an RE-123 system. Also note that TAFM is more prominent in the $Bi_2Sr_2CaCu_2O_8$ system than in RE-123 for similar reasons [11, 12].

It is also interesting to note that no direct correlation is observed between the T_c and TAFM broadening of resistivity in all the four samples, derived from the same host compound Er-123, depicted in figure 4. Although the Zn-substituted sample ($y = 0.1$, $x = 0.15$) has the lowest T_c (∼44 K), it still shows a TAFM broadening similar to the Zn-free sample ($x = 0$, $y = 0.1$) with the highest T_c (∼77 K) (see figures 4(a) and (c)), whereas the Fe-substituted sample ($y = 0.1$, $x = 0.15$), which has a comparable T_c (∼74 K) to the latter sample, shows a larger TAFM broadening (see figures 4(a) and (d)). A similar conclusion can be drawn for the Zn/Fe-free ($x = 0$) Ca-substituted samples with $y = 0.1$ and 0.2 discussed earlier. These results reveal that properties such as anisotropy, disorder and electronic structure can be more dominant, compared to T_c alone, in determining the FLL dynamics of an HTSC material.

Finally, note the presence of hump-like structures in all the $R(T)$ presented in figure 4. This structure was found to be more prominent in the series of samples with $y = 0.1$ (figure 4(a)) than in the series with $y = 0.2$ (figure 4(b)). The observed hump in the presence of a magnetic field may not be necessarily related to its presence when $B = 0$ (see, e.g., figure 4(a)). This is demonstrated by the Fe-substituted sample, where the hump is missing when $B = 0$ and appears only in the presence of a magnetic field (see figure 4(d)). Similar humps in melt-processed NdEuGd-123 have been attributed to site-dependent disorder and pinning effects in [14]. The pinning generated by the disorder due to Ca and/or Fe/Zn substitution in the Er-123 system can thus be a possible reason for the observed $R(T)$ humps in a magnetic field.

3.4. Possible effects of the ceramic nature of the samples

The samples studied in this work were prepared by the standard solid-state reaction and sintering route that is well known to result in a ceramic-like HTSC material. In the discussion so far we have not taken into account the inter-granular microstructure of the samples and the possible effects of the same on the various results obtained in the present work. The possible factors that could have affected the results extrinsically can broadly be sample density, texturing, segregation of the dopants at grain boundaries, inhomogeneity and weak links. Before we discuss them, we mention that the chosen range of concentrations for various dopants in the present work, i.e. $0 \leqslant x \leqslant 0.2$ and $0 \leqslant y \leqslant 0.2$ for $Er_{1-y}Ca_yBa_2Cu_{3-x}(Fe, Zn)_xO_{7-\delta}$, is well within the solubility regimes reported for them [3, 4, 15–21].

First, the measured densities of the samples show no systematic change with either x or y in either Fe and Zn. For all the samples the density varies randomly between 5.5–6.1 g cm^{-3}. Thus none of the studied properties can be directly linked with the sample density. For instance, the
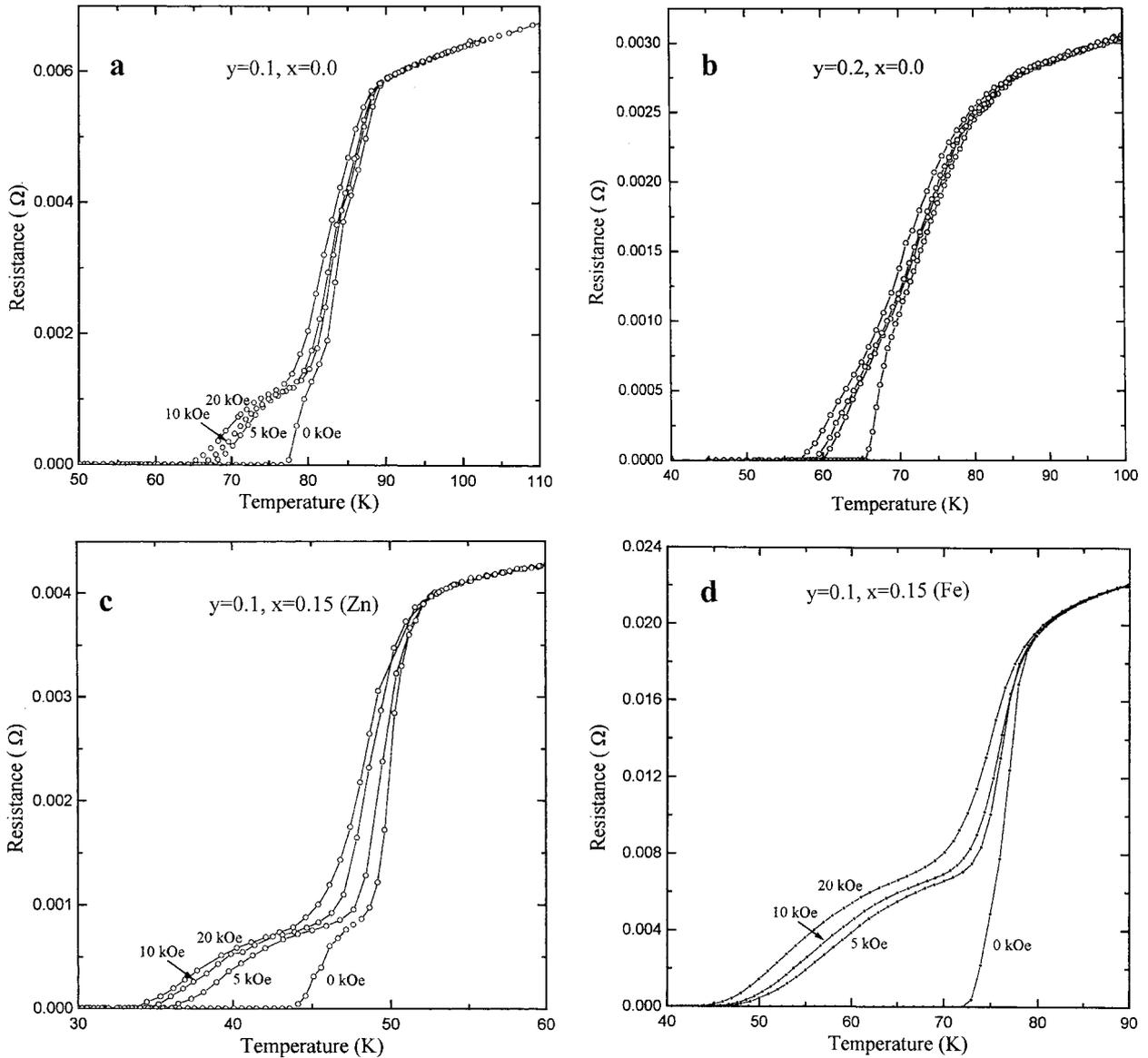
Figure 4. Resistance as a function of temperature in the presence of applied magnetic field for $Er_{1-y}Ca_yBa_2Cu_{3-x}(Fe, Zn)_xO_{7-\delta}$ samples: (a) $y = 0.1$, $x = 0$; (b) $y = 0.2$, $x = 0$; (c) $y = 0.1$, $x = 0.15$ (Zn); and (d) $y = 0.1$, $x = 0.15$ (Fe).

behaviour of the density is inconsistent with the change in room temperature resistivity (ρ_{RT}) as a function of both x and y for both Fe and Zn as depicted in figure 6. The observed systematic change in ρ_{RT} with x supports the previous [18, 19, 21] findings that even in polycrystalline HTSC samples ρ_{RT} depends on several intrinsic parameters such as disorder and change in electronic structure due to dopant addition. Another interesting property is the measured decrease in micro-hardness with increasing Fe and Zn content in Er(Ca)-123 (see figure 3). For both series of (ceramic) samples the micro-hardness results may apparently reflect a decrease in density, which is not true. This definitely suggests that Fe/Zn substitution changes the material and, in particular, the intra-granular shear modulus, which determines the plastic deformation of the grains in the samples. The net effect may be that the hardness goes down. It is worth pointing out that the copper–oxygen networks in the present crystal structure are very densely packed planes of the unit cell and consequently the shear modulus is expected

to change significantly when they are doped with Zn or Fe, as in the present case.

Second, with a change in x and y, we did not observe any anomalous enhancement of the 00l peaks in the XRD patterns, that rules out the possibility of texturing with increased dopant addition. Third, when the dopants had segregated at the grain boundaries in all the samples, the $T_c(x, y)$ should not have shown the expected [3, 4, 15–20] change. Fourth, within the limits of XRD, typically 3%, no reflections pertaining to impurities are observed in any of the samples. However, for $B = 0$, the fact that the superconducting transition to $R = 0$ in all samples is broad (see figure 4) does indicate the presence of inhomogeneity and/or weak links at the grain boundaries.

The main issue in the present paper is the broadening of the transition in the presence of a high dc magnetic field, and a comparison of the same in samples with various dopants. We now illustrate that the presence of inhomogeneity and/or weak
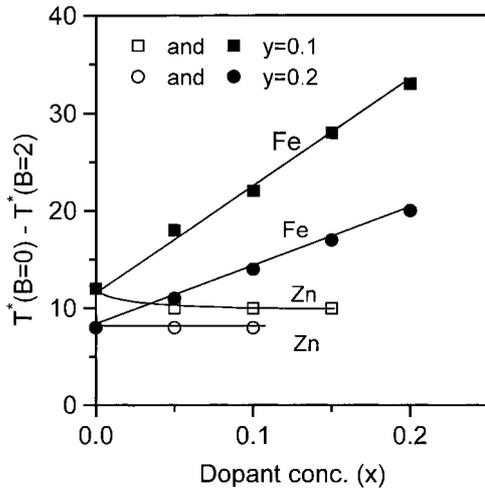
Figure 5. Shift in T^* as a function of Ca, Fe and Zn content in $Er_{1-y}Ca_yBa_2Cu_{3-x}(Fe,Zn)_xO_{7-\delta}$.
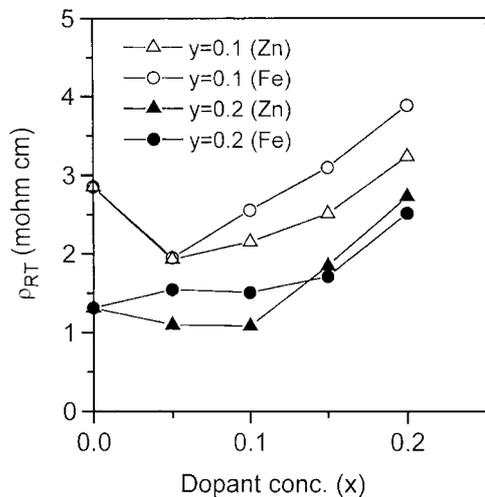
Figure 6. Resistivity (at 300 K) as a function of Fe/Zn content in $Er_{1-y}Ca_yBa_2Cu_{3-x}(Fe,Zn)_xO_{7-\delta}$ with $y = 0.1$ and 0.2.

links does not actually alter the interpretation of the high dc field $R(T, B)$ data of our samples in terms of TAFM.

(1) Note that for $B = 0$ in the Zn-based sample ($y = 0.1$, $x = 0.15$) the transition width ~7 K (see figure 4(c)) is higher than that observed (~4 K, see figure 4(d)) for the Fe-based sample ($y = 0.1$, $x = 0.15$), whereas in the presence of a field, e.g. for $B = 20$ kOe, the former shows a much smaller (~10 K, see figure 4(c)) transition broadening than that observed (~28 K, see figure 4(d)) in the latter. This itself reveals that TAFM dominates over any other factor (inhomogeneity/weak links) in determining the broadening of the resistive transition in high magnetic fields.

(2) The resistive transitions in superconducting ceramics at typically small currents are known to result in the actual T_c of well-connected grains [22]. Note that typical weak-link J_c values reported for RE-123 ceramics are around 200 A cm^{-2} for $B = 0$ to 300 Oe at 77 K [23]. Use of very small current densities (10 mA cm^{-2}) in the present work ensures that $T_c(R = 0)$ is measured in the zero current limit. The current density was changed by a factor of five

in some of our samples (chosen randomly) and no appreciable change (within ± 1 K) was observed in $T_c(R = 0)$.

(3) In high dc fields, i.e. $B > 300$–3000 Oe [22, 23], the weak links are quenched and the measured properties such as J_c and flux motion are representative of well-connected/intra-grain behaviour.

In the light of these facts, we feel that the present analysis of various dopants with respect to the host samples is justified as far as TAFM is concerned.

4. Conclusions

In the present work we have reported the effect of Fe/Zn substitution in the Er(Ca)-123 system on various properties such as grain size, hardness and the FLL dynamics. XRD showed that the presence of Ca in Er-123 system does not alter the effect of Fe or Zn substitution which was already known in the case of the pure Er-123 system. The grain size was found to decrease with increase in both Fe and Zn; however, the effect was more dominant in the former case. The micro-hardness that was found to decrease with both Fe and Zn substitution cannot be understood by the change in the grain size alone, and may indicate a change in the shear modulus of the respective material. Several conclusions were reached by the observed TAFM broadening of resistive transitions:

(1) an increase in the Ca content in the Er(Ca)-123 system leads to an increase in pinning barrier;
(2) substitution of Fe (at the Cu(1)-site in Cu–O chains) leads to an enhancement of TAFM compared to Zn substitution (at the Cu(2)-site in CuO$_2$ planes) that has no effect on TAFM; and
(3) the effect of various substitutions on the parameters such as anisotropy, disorder and electronic structure can be more dominant, compared to the change in T_c, in determining the FLL dynamics.

Acknowledgments

References

[1] Blatter G, Feigelman M V, Geshkenbein V B, Larkin A I and Vinokur V M 1992 *Rev. Mod. Phys.* **66** 1125
[2] Nelson D R and Vinokur V M 1993 *Phys. Rev.* B **48** 13 060
[3] Narlikar A V, Rao C V N and Agarwal S K 1989 *Studies of High Temperature Superconductors* vol 1, ed A V Narlikar (New York: Nova) p 341
[4] Tarascon J M and Bagley B G 1993 *Chemistry of Superconductor Materials* ed T A Vanderah (New Jersey: Noyes) p 310
[5] Tallon J L, Bernhard C, Shaked H, Hitterman R L and Jorgensen J D 1995 *Phys. Rev.* B **51** 12 911
[6] Murakami M, Sakai N, Higuchi T and Yoo S I 1996 *Supercond. Sci. Technol.* **9** 1015

[7] Yamauchi H, Karppinen M, Ito T, Suematsu H, Matsuura M and Isawa K 1998 *Supercond. Sci. Technol.* **11** 1006

[8] Tallon J L, Williams G V M and Loram J W 2000 *Physica* C **338** 9

[9] Hammerl C, Schmehl A, Schulz R R, Goetz B, Bielefeldt H, Schneider C W, Hilgenkamp H and Mannhart J 2000 *Nature* **407** 162

[10] Farneth W E, Bordia R K, McCarron III E M, Crawford M K and Flippen R B 1988 *Solid State Commun.* **66** 953

[11] Palstra T T M, Batlogg B, van Dover B, Schneemeyer L G and Waszczak J V 1988 *Phys. Rev. Lett.* **61** 1662

[12] Palstra T T M, Batlogg B, van Dover B, Schneemeyer L F and Waszczak J V 1989 *Phys. Rev.* B **41** 6621

[13] Bandyopadhyay A K, Varandani D, Gmelin E and Narlikar A V 1994 *Phys. Rev.* B **50** 462

[14] Pradhan A K, Muralidhar M, Koblischka M R, Murakami M and Nakao K 1999 *Appl. Phys. Lett.* **75** 253

[15] Tarascon J M, Barboux P, Miceli P F, Greene L H, Hull G W, Eibschutz M and Sunshine S A 1988 *Phys. Rev.* B **37** 7458

[16] Manthiram A and Goodenough J B 1989 *Physica* C **159** 760

[17] Xu Y, Sabatini R L, Moodenbaugh A R, Zhu Y, Shyu S G, Suenaga M, Dennis K W and McCallum R W 1990 *Physica* C **169** 205

[18] Cooper J R, Obertelli S D, Freeman P A, Zheng D N, Loram J W and Liang W Y 1991 *Supercond. Sci. Technol.* **4** S277

[19] Zagoulaev S, Monod P and Jegoudez J 1995 *Phys. Rev.* B **52** 10 474

[20] Sedky A, Gupta A, Awana V P S and Narlikar A V 1998 *Phys. Rev.* B **58** 12 495

[21] Awana V P S, Agarwal S K, Das M P and Narlikar A V 1992 *J. Phys.: Condens. Matter* **4** 4971

[22] Kupfer H, Apfelstedt I, Flukiger R, Keller C, Meier-Hirmer R, Runtsh B, Turowski A, Wiech U and Wolf T 1988 *Cryogenics* **28** 950

[23] Ekin J W, Larson T M, Hermann A M, Sheng Z Z, Togano K and Kumakra H 1989 *Physica* C **160** 489